Quaternary Research 79 (2013) 24–36

Contents lists available at SciVerse ScienceDirect

Quaternary Research

journal homepage: www.elsevier.com/locate/yqres

Using fire regimes to delineate zones in a high-resolution lake sediment record from the western United States

Jesse L. Morris [a,*], Andrea Brunelle [b], R. Justin DeRose [c], Heikki Seppä [a], Mitchell J. Power [b,d], Vachel Carter [b], Ryan Bares [b]

[a] Department of Geosciences and Geography, University of Helsinki, 00014 Helsinki, Finland
[b] Department of Geography, University of Utah, Salt Lake City, UT 84112, USA
[c] USDA Forest Service, Forest Inventory Analysis, Rocky Mountain Research Station, Ogden, UT 84401, USA
[d] Utah Museum of Natural History, Garrett Herbarium, University of Utah, Salt Lake City, UT 84112, USA

ARTICLE INFO

Article history:
Received 20 February 2012
Available online 10 November 2012

Keywords:
Charcoal
Fire regime
Fire season
Forest disturbance
Lake sediments
Pollen
Paleoecology
Regime shift
Spruce-fir forest
Wildfire

ABSTRACT

Paleoenvironmental reconstructions are important for understanding the influence of long-term climate variability on ecosystems and landscape disturbance dynamics. In this paper we explore the linkages among past climate, vegetation, and fire regimes using a high-resolution pollen and charcoal reconstruction from Morris Pond located on the Markagunt Plateau in southwestern Utah, USA. A regime shift detection algorithm was applied to background charcoal accumulation to define where statistically significant shifts in fire regimes occurred. The early Holocene was characterized by greater amounts of summer precipitation and less winter precipitation than modern. Ample forest fuel and warm summer temperatures allowed for large fires to occur. The middle Holocene was a transitional period between vegetation conditions and fire disturbance. The late Holocene climate is characterized as cool and wet reflecting an increase in snow cover, which reduced opportunities for fire despite increased availability of fuels. Similarities between modern forest fuel availability and those of the early Holocene suggest that warmer summers projected for the 21st century may yield substantial increases in the recurrence and ecological impacts of fire when compared to the fire regime of the last millennium.

© 2012 University of Washington. Published by Elsevier Inc. All rights reserved.

Introduction

Recent episodes of historically unprecedented tree mortality suggest that forest ecosystems in western North America (WNA) are undergoing substantial and rapid reorganization (Williams et al., 2010). Forest disturbance regimes are decoupling from historic norms due to warming temperatures, advancing spring snowmelt, and increasing aridity that are resulting in novel ecological outcomes and states (Scheffer et al., 2001; Westerling et al., 2006; Raffa et al., 2008). Long-term ecological records, such as those reconstructed from sediments archived in lakes, offer key insights into abrupt changes in climate and disturbance regimes. During the coming century, new ecological challenges will require a re-evaluation of land stewardship policies that will benefit greatly from consideration of longer term ecological records (Willis and Birks, 2006).

Because fire is a keystone ecological process across a diversity of landscapes, the fire-regime concept is often emphasized as a common and accessible construct for interdisciplinary discourse (Falk and Swetnam, 2003; Conedera et al., 2009; Whitlock et al., 2010). Fire regimes are timescale-dependent, and therefore may include numerous biotic and abiotic attributes to describe fire variability (Whitlock et al., 2010). Over longer temporal scales, fire regimes are responsive to insolation variability, climate dynamics, human pressures, and forest composition (Power et al., 2008, 2012). Here we define "fire regime" as the disturbance characteristics of fire frequency and severity over centennial to millennial timescales.

Recent advances in quantitative techniques used to reconstruct wildfire from lake sediments include quantitative biomass metrics (Marlon et al., 2006; Seppä et al., 2009); compilation of the Global Palaeofire Database (Power et al., 2010); statistical decomposition and peak detection schemes (Long et al., 1998; Higuera et al., 2010); paired proxy approaches using historical records, tree rings, and lake sediments (Higuera et al., 2011); charcoal dispersion models (Higuera et al., 2007); and circumspect laboratory, field, and site selection protocols (Whitlock and Millspaugh, 1996; Whitlock and Larsen, 2001; Ali et al., 2009).

Building on these advances, we apply a regime shift detection algorithm to determine where statistically significant shifts in charcoal accumulation occur (Rodionov, 2004). We characterize these shifts as a switch in fire regimes attributable to climate-mediated changes in vegetation structure and composition. We elected to examine the paleoecological reconstruction presented here through the lens of wildfire because of the ecologically isolated location of our study site. This condition allows us to discount the possibility of immigration of fire-prone or fire-adapted species, known in many regions to be an important catalyst

* Corresponding author.
E-mail address: jesse.morris@helsinki.fi (J.L. Morris).

0033-5894/$ – see front matter © 2012 University of Washington. Published by Elsevier Inc. All rights reserved.
http://dx.doi.org/10.1016/j.yqres.2012.10.002

for fire regime shifts (e.g., Lynch et al., 2004; Ohlson et al., 2011). In our analysis, we assume that climate-driven changes to forest structure, fuel moisture, and fire-season length are dominant controls on fire recurrence and magnitude.

In this lake-sediment reconstruction we use charcoal to delineate stratigraphic zones. Stratigraphic records are typically analyzed using clustering, binary, or optimal statistical approaches to identify periods of similar (or uniform) pollen composition (Grimm, 1987; Ritchie, 1995; Bennett, 1996). However, these approaches implicitly assume that plant diversity and/or changes in plant community composition are the primary objective(s) of the reconstruction. At most sites, the pollen assemblage provides a minimum estimate of the surrounding plant communities, under-representing species present by an order of magnitude (Ritchie, 1995). Furthermore, the reliability and representativeness of zones are often influenced by the temporal resolution of pollen samples, which may vary considerably within a single core and among sites (Bennett, 1996). On the other hand, stratigraphic charcoal records can be analyzed efficiently at every contiguous centimeter and are representative of climate effects on biomass and forest stand conditions. In ecologically isolated landforms, such as sky islands in southwestern USA, the immigration of novel species into upland forests is improbable due to vast expanses of *Artemisia* (sagebrush) steppe at lower elevations that has persisted across the southwest since at least the Pleistocene (Davis, 1990; Davis and Pitblado, 1995). Therefore, delineating biostratigraphic zones using a pollen assemblage may be less useful in these and similar ecosystems. In contrast to pollen records, charcoal records from these sky island ecosystems exhibit considerable variability and can be used to characterize time-transgressive reorganizations of vegetation and fuel structure (Morris, 2011).

This sedimentary charcoal reconstruction is the first high-resolution fire history for the Markagunt Plateau ("Markagunt," here after) (Fig. 1a). Information about the long-term role of fire on the Markagunt is of great interest because numerous private residences and commercial structures, including the Brian Head Ski Resort, exist within a matrix of federally managed wildland. In this paper we describe Holocene

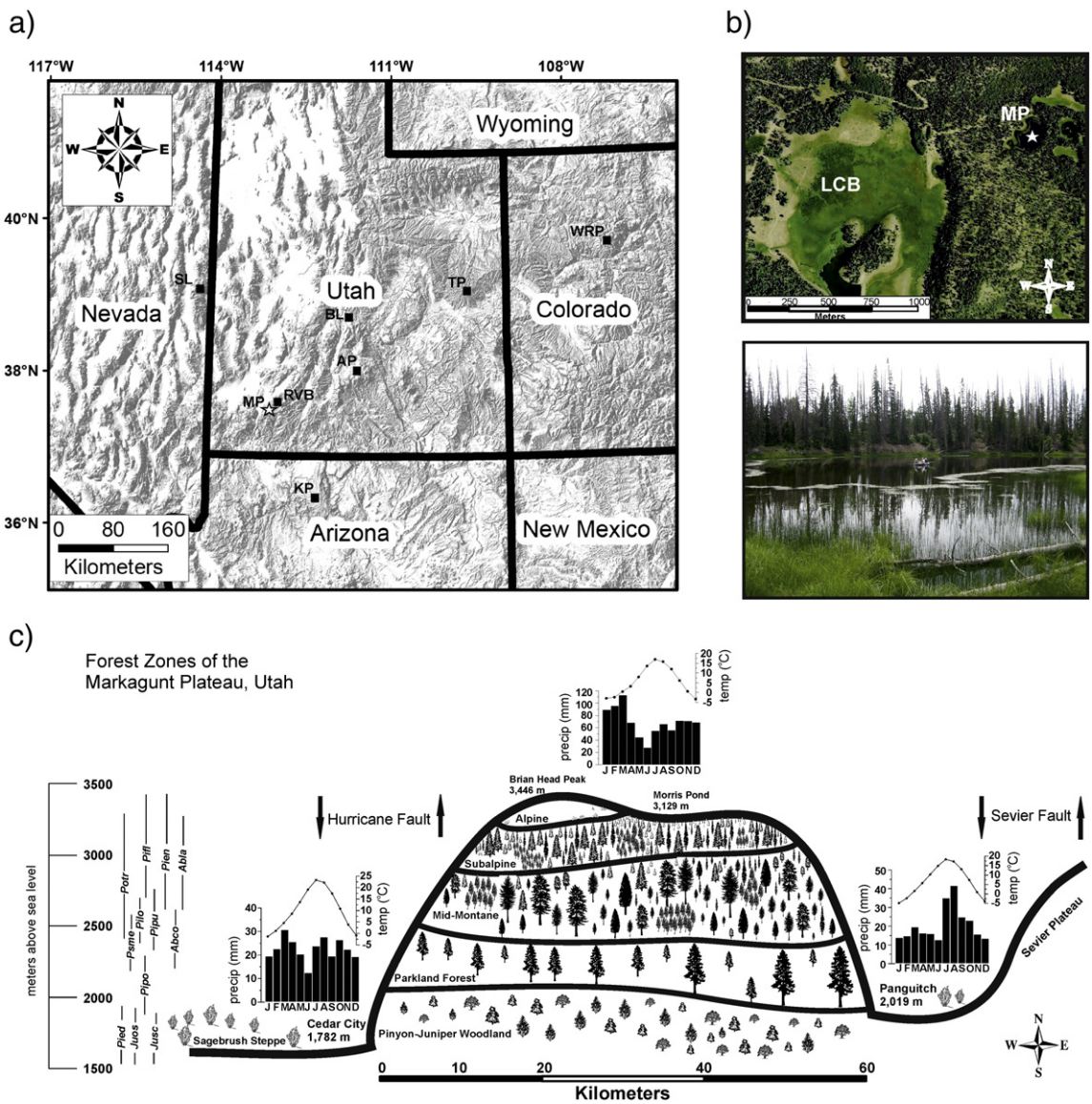

Figure 1. a) Map of the western United States depicting the location of the Markagunt Plateau (☆) and other sites discussed herein (■): BL = Blue Lake (Morris et al., 2010), KP = Kaibab Plateau (Weng and Jackson, 1999), AP = Aquarius Plateau (Morris and Brunelle, 2012), RVB = Red Valley Bog (Madsen et al., 2002), SL = Stella Lake (Reinemann et al., 2009), TP = Tavaputs Plateau (Knight et al., 2010), and WRP = White River Plateau,(Anderson, 2011, 2012). b) Images of Lowder Creek Bog (LCB) (Anderson et al., 1999) and Morris Pond (MP) (this study) sites; ☆ indicates approximate location where sediment cores were collected. c) Schematic representation of forest zones and climagraphs depicting relationships among key forest taxa, precipitation, and temperature versus elevation.

vegetation conditions and fire regimes, and address the following questions: (1) What is the role of millennial-scale climate forcing on wildfire dynamics on the Markagunt? (2) How do changes in the vegetation community structure and composition affect fire recurrence and peak magnitude? (3) How does this high-resolution charcoal and pollen record agree with other Holocene paleoecological reconstructions in the region?

Study area

Regional setting—southern Utah

The Colorado Plateau is a topographically complex geologic province identified as an important physiographic and ecological crossroads (Anderson et al., 2000). Subalpine landforms of the Colorado Plateau receive significant growing season precipitation via the North American Monsoon (NAM) and during the winter from Pacific frontal storms (Mock, 1996; Adams and Comrie, 1997). Despite broad seasonal trends across the region, monthly precipitation maxima are heterogeneous and elude strict classification due to the effects of complex topography and steep elevation gradients (Mock, 1996). The primary driver of winter precipitation is El Niño–Southern Oscillation (ENSO) (Ropelewski and Halpert, 1986; McCabe and Dettinger, 1999). ENSO status is described as positive (or negative) indicating warm (or cool) sea surface temperatures in the southern Pacific Ocean. During an El Niño episode the southwestern USA generally receives greater-than-average winter precipitation, whereas arid cold-season conditions prevail during La Niña. Based on a sedimentary reconstruction at Laguna Pallcacocha in southern Ecuador, Moy et al. (2002) provide evidence of long-term ENSO frequency and intensity. Long-term ENSO variability generally has increased over the course of the Holocene. The Pacific Decadal Oscillation (PDO) is somewhat similar in terms of climate and circulation response for western North America, though the PDO exhibits a 20–30 yr period and describes SST conditions in the northern Pacific Ocean as positive (or negative) in reference to warm (or cool) temperatures (Mantua et al., 1997). Given the comparatively low temporal frequency of PDO, its status can enhance (constructive) or suppress (destructive) winter precipitation in WNA during El Niño and La Niña events (McCabe and Dettinger, 1999; Biondi et al., 2001; Wise, 2010). In southern Utah, the greatest occurrence and risk of wildfire that have been observed and modeled are during La Niña episodes and negative-phase PDO (Schoennagel et al., 2005; Brown et al., 2008).

The subalpine plateaus and tablelands (i.e., "sky islands") of the Colorado Plateau encompass an area of ca. 30,000 km^2, and these uplifted landforms occur in three primary orogenic belts (Arno and Hammerly, 1984; Anderson et al., 2000). These features include nine named 'high plateaus' oriented northeast–southwest, separated by deep valleys (Arno and Hammerly, 1984). In general, the highlands are forested and vegetation communities more closely resemble those of the Rocky Mountains than the Great Basin or Sierra Nevada (Arno and Hammerly, 1984). Vegetation zones of the Colorado Plateau are stratified by elevation along environmental gradients and are summarized in Figure 1c.

Markagunt Plateau

The Markagunt trends northeast–southwest and covers an area of 2100 km^2 with an average elevation of 3320 m. It is the westernmost landform of the Colorado Plateau and forms the hydrologic and physiographic boundary with the Great Basin. Gregory (1949) sums the geologic setting of the Markagunt as "a lofty, eastward-tilted earth-block whose original surface has been considerably reduced by erosion, remodeled by volcanism, and slightly modified by glaciations." Surficial bedrock on the Markagunt is a mosaic of Holocene-age basalt lava and carbonate-rich Late Paleocene to Eocene-age Claron Formation (Gregory, 1949; Goldstrand, 1994). On the southern Markagunt is a vulcanokarst (see Ford and Williams, 2007) landscape with numerous dissolution features that drain the upland landscape rapidly and elevate drought susceptibility (Wilson and Thomas, 1964).

Morris Pond (MP) (37°40.48′N, 112°46.49′W) occurs at 3126 m elevation with a surface area of 1 ha in the Lowder Creek watershed (Fig. 1b). MP is fed by subaerial springs and has no surface inlet or outlet. MP exists near the terminus of the extinct (Pleistocene) Lowder Creek Glacier in a small, ice-block depression between two steeply sloped embankments (Mulvey et al., 1984). MP is currently surrounded by a dense *Picea engelmannii* - *Abies lasiocarpa* forest that experienced severe mortality of *P. engelmanni* from a *Dendroctonus rufipennis* (spruce beetle) epidemic during the AD 1990s (DeRose and Long, 2007; Morris and Brunelle, 2012). Two low-resolution paleoenvironmental reconstructions exist from the Markagunt, including Lowder Creek Bog (LCB) (Anderson et al., 1999) and Red Valley Bog (2822 m) (Madsen et al., 2002).

Materials and methods

Field work

Sediment cores were collected at MP using a platform anchored over the deepest area of the pond (1.5 m water depth) where sediment focusing would ensure maximum sediment recovery. A 74-cm core (MP08A) of the unconsolidated upper sediments was collected using a modified Klein coring device in August 2008. In August 2009, a 4.82-m sediment core (MP09B) was retrieved using a modified Livingstone piston corer.

Core lithology

The MP sediments are composed primarily of light-to-dark brown organic gyttja, with dark organic bands conspicuous in the lower core (Fig. 2). Despite the small, steeply sloped catchment surrounding MP (<5 ha), the pond has a remarkably high, yet stable, sedimentation rate over the Holocene averaging 0.5 mm/yr (Fig. 2). However, this sedimentation rate is similar to other small, spring-fed ponds found in karst landscapes in this region (Morris, 2011; Lundeen, 2012). The sediments did not appear laminated in any portion of the core.

Chronology

A chronology for the upper 24 cm of MP08A was established by analyzing for ^{210}Pb/^{137}Cs (Fig. 2; Table 1). Subsamples were weighed and then dried in a muffle furnace at 100°C to remove moisture. Dehydrated samples were submitted for analysis to the USGS Laboratory in Denver, CO. The ^{210}Pb record was interpreted using AD 1963 as the peak in ^{137}Cs associated with climax of atmospheric detonation of nuclear test weapons. The top cm was assigned to the year of core retrieval for age-model reconstruction. The short core was linked to the long core by matching discrete peaks in charcoal accumulation.

Accelerator mass spectrometry (AMS) ^{14}C dates were obtained from pollen residues isolated from the MP sediments (Fig. 2; Table 1). For each sample, one cm^3 of sediment was treated with a series of non-organic chemical rinses to isolate pollen, using the Schulze technique (Kapp et al., 2000). Pollen isolate samples were submitted to the Center for Applied Isotope Studies at the University of Georgia for analysis. Previous analyses comparing AMS dates on pollen isolations to macrofossils demonstrated that pollen dates provide a reliable chronology (Brunelle and Dvoracek, personal communication). AMS results were converted from ^{14}C years to calendar years before present (cal yr BP) using the INTCAL09 calibration set in the Calib 6.0 module (Reimer et al., 2009). Age–depth relationships were determined using a smoothing spline software developed by Dr. Patrick Bartlein at the University of Oregon (see also Marlon et al., 2008; Power et al., 2008, 2012). The spline was calculated with a smoothing parameter (spar) of 0.6, a lambda (λ) of 1.590001e-06, and equivalent degrees of freedom (d.f.) of 7.428927.

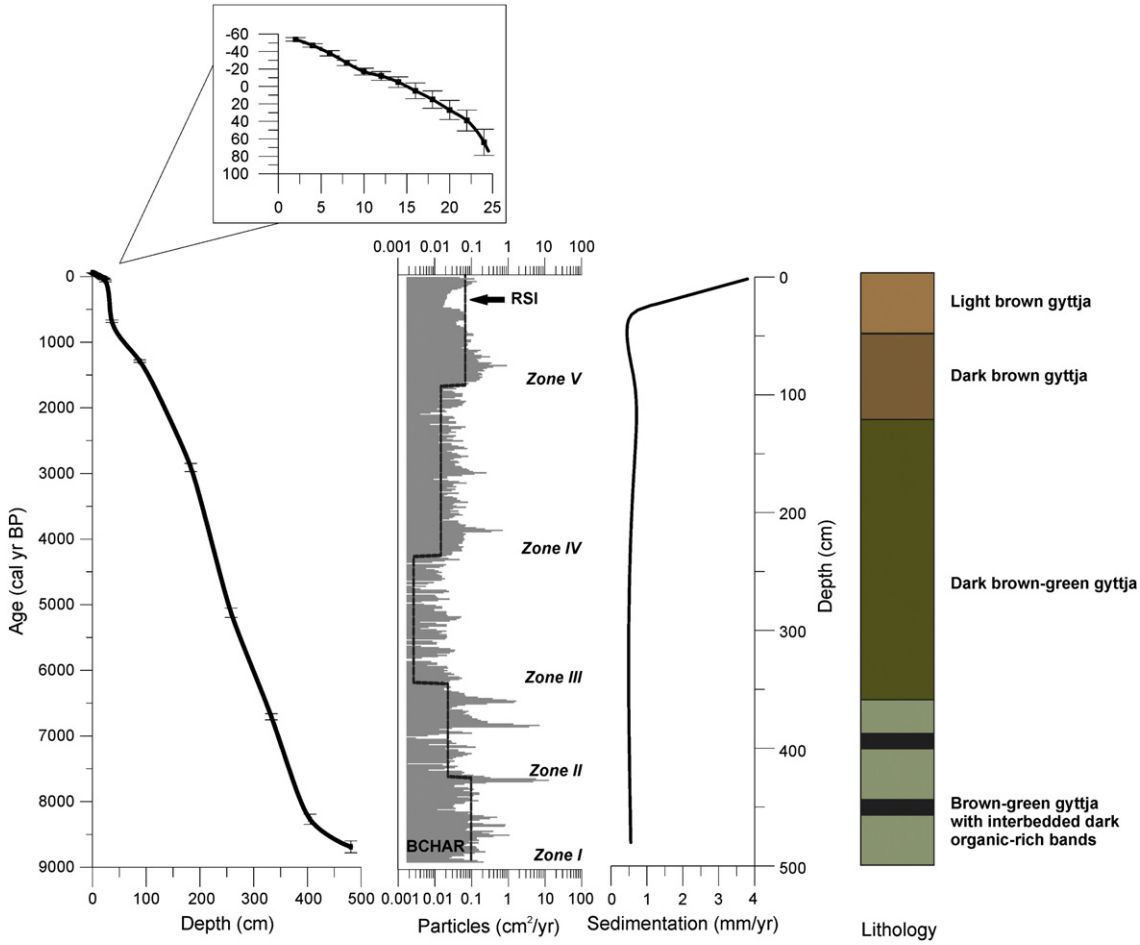

Figure 2. Plots of age model, stratigraphic zones delineation based on regime shifts (RSI) of background charcoal (BCHAR), sedimentation rate, and core lithology. Age model plot depicts calibrated AMS ^{14}C ages and ^{210}Pb (inset) versus depth plots. Present is defined as AD 1950. Table 1 summarizes age assignments. Table 2 summarizes charcoal zones.

Table 1
Summary of laboratory results and age–depth assignments for Morris Pond chronology.

Depth (m)[a]	Core ID	^{14}C age ± 1σ[b]	2σ age range (cal yr BP)[c]	Relative area under distribution	Assigned ^{210}Pb age (yr AD)[d]	Assigned age (cal yr BP)	Material dated	Lab ID number
0.00	MP09A				2009 ± 0[e]	−59		
0.02	MP09A				2004 ± 2	−54	Gyttja	MP09A0102
0.04	MP09A				1997 ± 2	−47	Gyttja	MP09A0304
0.06	MP09A				1988 ± 2	−38	Gyttja	MP09A0506
0.08	MP09A				1977 ± 3	−27	Gyttja	MP09A0708
0.10	MP09A				1967 ± 3	−17	Gyttja	MP09A0910
0.12	MP09A				1962 ± 4	−12	Gyttja	MP09A1112
0.14	MP09A				1955 ± 5	−5	Gyttja	MP09A1314
0.16	MP09A				1945 ± 6	5	Gyttja	MP09A1516
0.18	MP09A				1935 ± 9	15	Gyttja	MP09A1718
0.20	MP09A				1923 ± 10	27	Gyttja	MP09A1920
0.22	MP09A				1911 ± 11	39	Gyttja	MP09A2324
0.24	MP09A				1886 ± 12	64	Gyttja	MP09A2123
0.36	MP09A	738 ± 20	660–699	0.996		680	Pollen	7045
0.88	MP08B	1360 ± 20	1270–1306	1.000		1288	Pollen	7044
1.83	MP08B	2804 ± 25	2846–2971	1.000		2909	Pollen	7046
2.58	MP08B	4516 ± 26	5051–5192	0.674		5122	Pollen	7863
3.33	MP08B	5893 ± 25	6661–6755	0.949		6708	Pollen	7047
4.05	MP08B	7452 ± 29	8192–8347	1.000		8270	Pollen	7864
4.81	MP08B	7901 ± 28	8598–8780	0.906		8689	Pollen	6096

[a] Depth below the sediment–water interface.
[b] AMS ^{14}C age determinations from Center for Applied Isotope Studies (CAIS) at the University of Georgia.
[c] ^{14}C ages calibrated to calendar years before present (cal yr BP) with INTCAL09 in Calib 6.0 (Reimer et al., 2009).
[d] $^{210}Pb/^{137}Cs$ ages from USGS Denver determined by Constant Rate of Supply (Appleby et al., 1979) adjusted for AD 1963 ^{137}Cs peak.
[e] Core top sample assigned to year of core retrieval.

Pollen analysis

Pollen subsamples (1 cm^3) were processed and analyzed at 4-cm intervals following methods described by Faegri et al. (1989). *Lycopodium* (clubmoss), an exotic spore in western North America, was introduced to each sample as a marker during processing. Slide-mounted pollen samples were examined using light microscopy at 500× magnification and counted to a minimum of 300 terrestrial grains. Grain identification was aided by laboratory reference collections and dichotomous keys (Erdtman, 1952; Bassett et al., 1978; Kapp et al., 2000). Pollen from desert taxa, including Chenopodiaceae (Goosefoot family, Amaranthaceae family sensu stricto) and Ephedraceae (Ephedra family), were subtracted from subalpine pollen totals listed in Table 2, but are included in Figures 3 and 5 and discussed in the text below. Differentiation among *Pinus* grains was based on the presence or absence of verrucae on the leptoma to distinguish diploxylon (yellow pine) from haploxylon (white pine). A considerable amount of *Pinus* grains was mechanically damaged, perhaps during processing, and diagnostic verrucae were lacking. Of the *Pinus* grains that were identifiable, the vast majority were haploxylon-type. Because much of the *Pinus* pollen was not able to be confidently differentiated, we chose to present these data as Total *Pinus*. Most identified *Pinus* grains were haploxylon, and therefore we suspect that this pollen type is largely representative of *Pinus flexilis*, but possibly some may represent pollen from *Pinus longaeva*. The closest modern population of *P. longaeva* occurs 5 km southwest of MP.

Pollen ratios were calculated using the equation $(a-b)/(a+b)$ and ratio data are presented in standard units (SU). The *Artemisia*/*Ambrosia* ratio is used as a proxy for the timing of growing season moisture availability. *Artemisia* prefers later seasonal arrival of precipitation while *Ambrosia* prefers moisture arriving earlier in the growing season (Maher, 1963; Cable, 1977). We propose that the *Artemisia*/*Ambrosia* ratio is a useful qualitative proxy for the NAM because a greater amount of late season precipitation from an intensified NAM would favor *Artemisia* over *Ambrosia* (higher ratio) and declining late season moisture would favor *Ambrosia* over *Artemisia* (lower ratio). The *Artemisia*/Chenopodiaceae (AC) ratio is commonly used as a qualitative proxy for past annual growing season moisture availability in arid and semi-arid regions because *Artemisia* requires more growing season moisture than Chenopodiaceae (Mensing et al., 2004; Herzschuh, 2007; Zhao et al., 2012).

Magnetic susceptibility, loss on ignition

Magnetic susceptibility (MS) data were collected for every contiguous centimeter of MP08A and MP09B to assess ferromagnetic mineral content of the sediments. Peaks in MS are associated with increased runoff and erosion from landscape disturbances such as logging and fire (Gedye et al., 2000). MS properties of MP08A sediments were determined using 10-cm^3 cups in the Bartington© coil sensor and of MP09B by placing long cores end-to-end and then passing the cores through a Bartington© ring sensor. Loss on ignition (LOI) analysis was performed on 1-cm^3 contiguous subsamples for MP08A and at 4-cm intervals for MP09B to assess organic and carbonate ($CaCO_3$) content of the sediment. Determination of organic and carbonate content was achieved by ignitions at 550°C and 900°C, respectively, for two hours (Dean, 1974).

Charcoal analysis

Subsamples for charcoal and macrofossil analysis (5–10 cm^3) were collected and analyzed for each contiguous cm and prepared following Whitlock and Millspaugh (1996). Sediment subsamples were screened through 125-μm and 250-μm nested sieves. Retrieved materials were placed on gridded petri dishes and then examined and counted using light microscopy at 40× magnification. These size fractions were selected because modern studies have shown that large particles do not travel far from their source and therefore most likely represent local (watershed-scale) fire history (Clark, 1988; Gardner and Whitlock, 2001). Charcoal counts for each sample were converted to concentration (particles/cm^3) and then calculated as influx (particles/cm^2/yr). To minimize variations in the record that might arise due to changes in sediment deposition rates, the concentrations were binned using the median sediment deposition time (25 yr). Newly binned concentrations were then converted to charcoal accumulation rates (CHAR, particles/cm^2/yr) and decomposed into background (BCHAR) and peak components (Higuera et al., 2009; http://CharAnalysis.googlepages.com). BCHAR is essentially the slowly varying trend in CHAR. Peaks (fire episodes) are determined as positive deviations from BCHAR, which we interpret as input of charcoal originating from a fire episode. Peaks were determined using a Lowess smoother which is robust to outliers within a 500-yr window width (Higuera et al., 2010). The background values for each time interval were then subtracted from the total CHAR accumulation for each

Table 2
Summary of pollen and charcoal data for each statistically significant fire regime zone.

Regime/age	BCHAR RSI[a]	FRI avg[b]	# of peaks[c]	Peak mag[c] range (avg)	Arboreal influx[d] and (percent)[e]						Shrub[f] influx[d] (percent)[e]	AP/NAP ratio[g] (avg)	Total terrestrial influx[d]
					Picea	*Abies*	*Pinus*	*Populus*	*Pseudotsuga*	Total			
Zone V modern–1800 cal yr BP	0.15	351	6	0.54–47.10 (9.04)	2276 (29%)	531 (7%)	1418 (18%)	219 (2%)	5 (<1%)	4449 (57%)	1273 (19%)	0.51	7583
Zone IV 1800–4200 cal yr BP	0.06	270	12	0.09–47.45 (5.83)	833 (23%)	63 (2%)	684 (19%)	62 (2%)	7 (<1%)	1649 (47%)	863 (24%)	0.30	3565
Zone III 4200–6200 cal yr BP	0.02	679	3	0.32–2.08 (1.40)	835 (24%)	45 (2%)	709 (21%)	57 (2%)	4 (<1%)	1650 (50%)	648 (20%)	0.42	3264
Zone II 6200–7700 cal yr BP	0.08	352	5	1.47–1068.38 (361.28)	1093 (28%)	35 (1%)	934 (23%)	77 (2%)	0	2139 (54%)	673 (18%)	0.47	3873
Zone I 7700–8600 cal yr BP	0.19	178	6	1.64–50.03 (25.07)	880 (21%)	73 (2%)	1216 (27%)	51 (1%)	2 (<1%)	2222 (52%)	879 (20%)	0.44	4295

[a] Background charcoal (particles/cm^2/yr) regime shift index (RSI) calculated using Student's *t*-test (Huber's WF = 5, P<.0001, cut-off = 100 yr) (Rodionov, 2004).
[b] Fire return interval (FRI) averaged (avg) for each zone.
[c] Peak detection and peak magnitude (particles/peak) determined using CharAnalysis (Higuera et al., 2009) and averaged (avg) for each zone.
[d] Pollen influx (grains/cm^2) averaged (avg) for each zone.
[e] Pollen percent (relative abundance).
[f] Includes all shrubs except desert taxa in Chenopodiaceae and Ephedraceae families.
[g] Ratio calculated as $(a-b)/(a+b)$ where a represents arboreal pollen (AP) and b represents non-arboreal pollen (NAP).

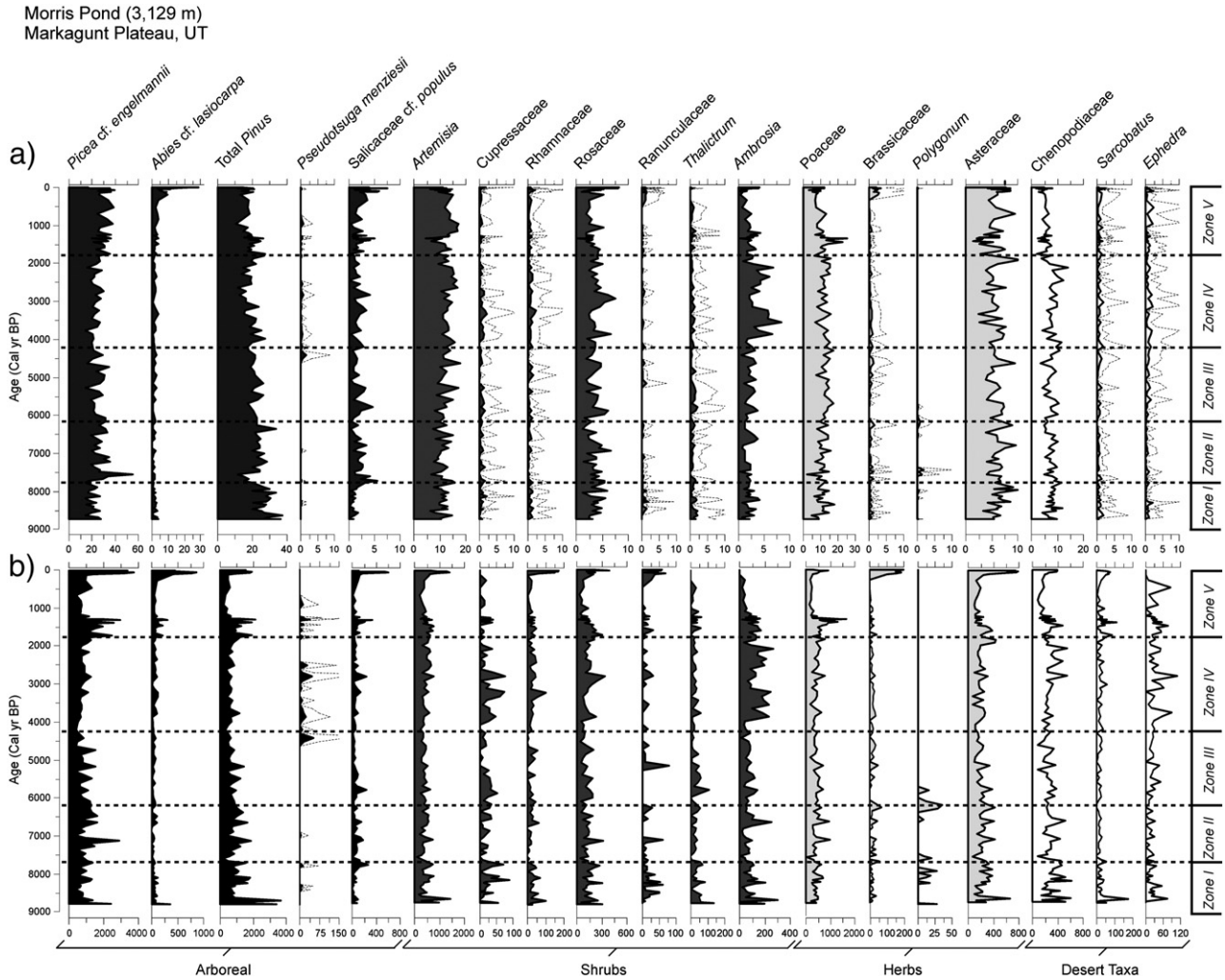

Figure 3. Pollen diagram for percentage (a) and influx (b) of selected taxa from Morris Pond. Note differing scales on x-axes. Dotted line plots indicate 5× exaggeration.

interval. The peaks in the charcoal record (i.e., intervals with CHAR values above BCHAR) were tested for significance using a Gaussian distribution, where peak CHAR values that exceeded the 95th percentile were considered significant. This procedure was applied for every 500-yr overlapping portion of the CHAR record, producing a unique threshold for each sample. Once identified, all peaks were screened to eliminate those that resulted from statistically insignificant variations in CHAR (Gavin et al., 2006). If the maximum count in a CHAR peak had a >5% chance of coming from the same Poisson-distributed population as the minimum charcoal count of the preceding 75 yr, then the peak was rejected (Higuera et al., 2010).

Fire regime zones

BCHAR variability results primarily from changes in fuel abundance (biomass) which is generally attributable to changes in climate (Whitlock et al., 2003; Marlon et al., 2006; Seppä et al., 2009). Because fire regimes are assumed to be responsive to adjustments in stable state conditions of the climate system, we applied a regime shift index (RSI) algorithm, incorporating a sequential Student's *t*-test (Huber's WF = 5, P < 0.0001, cut-off = 100 yr), to BCHAR to determine where statistically significant differences between mean values of two subsequent regimes occur to define zones, or 'tipping points,' in the MP record (Rodionov, 2004; http://www.beringclimate.noaa.gov/regimes/). The RSI determined where statistically significant, stepwise shifts in BCHAR occur. We identify these shifts as a fire regime zone (Fig. 2). Quantified fire regimes zones were then used to describe the MP record and enhance interpretation of climate influence on landscape conditions.

Results

Zone I: 8600–7700 cal yr BP

Pollen

The Zone I pollen assemblage includes abundant arboreal pollen (AP) (52%) with shrub (25%) and herb pollen (23%). AP in Zone I is dominated by *Pinus* (30%) with *Picea* (20%), *Abies* (2%), and *Populus* (2%) also represented (Fig. 3). Shrub pollen is composed predominantly of *Artemisia* (9%), Chenopodiaceae (8%), Rosaceae (3%), and *Ambrosia* (2%). Herbs are dominated by Poaceae (10%) and Asteraceae (6%). *Polygonum* and Ranunculaceae family pollen are also present (1–2%). *Polygonum* is particularly noteworthy because it occurs infrequently elsewhere in the record. Total pollen influx averages 4295 grains/cm^2 (Fig. 4). Aquatic algal spores are dominated by *Isoetes* (60 spores) which declines noticeably at 8200 cal yr BP (<10 spore) (Fig. 5).

Charcoal

Zone I BCHAR averages 0.2 cm^2/yr and fire return interval (FRI) averages 178 yr between burning episodes (most frequent of the record) (Fig. 4). Six discrete charcoal peaks occur in Zone I, with four peaks

clustered around 8200 cal yr BP. Peak magnitude for the five peak events ranges between 1.6 and 50.1 and averages 25.1 particles/peak.

Zone II: 7700–6200 cal yr BP

Pollen

Zone II pollen assemblage includes abundant AP (54%) with shrub (29%) and herb pollen (17%). *Picea* pollen composes the greatest amount of average AP (28%) with *Pinus* also important (23%) (Fig. 3). *Picea* pollen increases (15% to 55%) at 7500 cal yr BP while *Pinus* pollen decreases precipitously between 7700 and 7500 cal yr BP (30% to 4%). *Abies* is variable (0–2%) and *Populus* (2%) is consistently present. Predominant shrubs include *Artemisia* (10%), Chenopodiaceae (9%), Rosaceae (3%), and *Ambrosia* (2%). Herbs are dominated by Poaceae (11%) and Asteraceae (6%). Average total pollen influx is third highest of the record (3873 grains/cm^2/yr). Total shrub influx is the

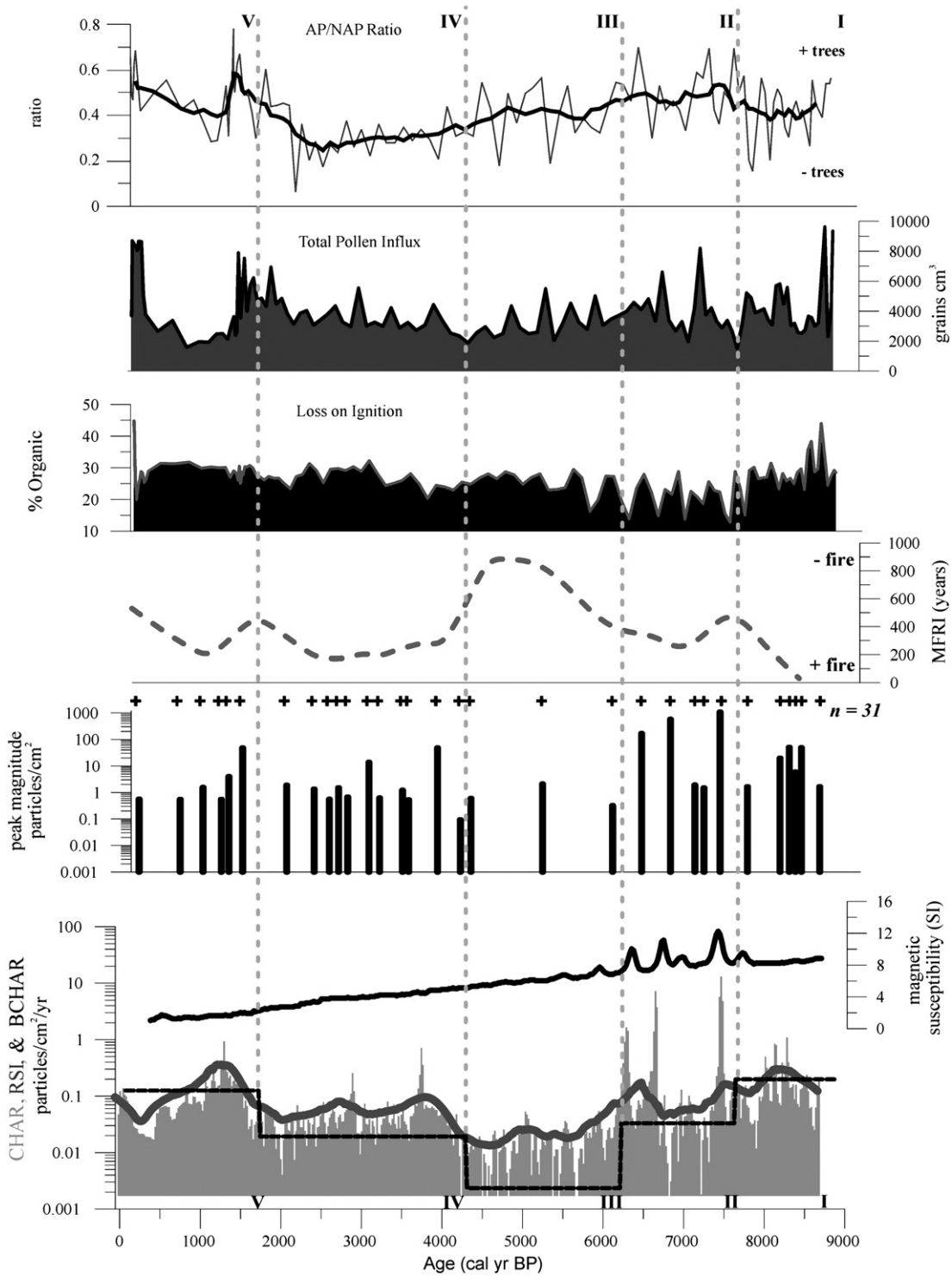

Figure 4. Pollen, geochemical, and charcoal data for Morris Pond. Note y-axis on charcoal figure plotted on log scale; + = peaks. BCHAR, peak magnitude, and fire-return interval were determined using CharAnalysis (Higuera et al., 2009). Dashed vertical lines indicate fire regime zones derived from regime shift index algorithm (RSI) (Rodionov, 2004).

lowest (673 grains/cm^2/yr) and total AP influx is second highest (2139 grains/cm^2/yr) (Fig. 4). Aquatic taxa are less abundant in Zone II than in Zone I. *Isoetes* is present in lower amounts (5–15 spores) and Cyperaceae are constant. Typhaceae is essentially absent. Sparse *Pediastrum* are present throughout Zone II, though there is a distinctive increase at 7400 cal yr BP (<60–80 spores/cm^2/yr) (Fig. 5).

Charcoal

Zone II BCHAR averages 0.1 cm^2/yr and FRI averages 352 yr (Fig. 4). Five discrete charcoal peaks occur in Zone II and are highest within the context of the entire record, ranging between 1.5 and 1068.4 and averaging 361 particles/peak.

Zone III: 6200–4200 cal yr BP

Pollen

Zone III pollen assemblage includes abundant AP (50%) with shrub (20%) and herb pollen (21%) less abundant. *Picea* pollen averages are the largest component of the arboreal community (24%) with *Pinus* also important (21%) (Fig. 3). *Abies* and *Populus* are variable between 2 and 4%. *Pseudotsuga menziesii* pollen enters the record near the termination of this zone. Predominant shrubs include *Artemisia* (14%), Chenopodiaceae (7%), Rosaceae (3%), and *Ambrosia* (3%). Rhamnaceae is consistently present during this period (2%). Herbs are dominated by Poaceae (12%) and Asteraceae (6%). Total pollen influx averages 3264 grains/cm^2/yr and is the lowest average of the five zones (Fig. 4).

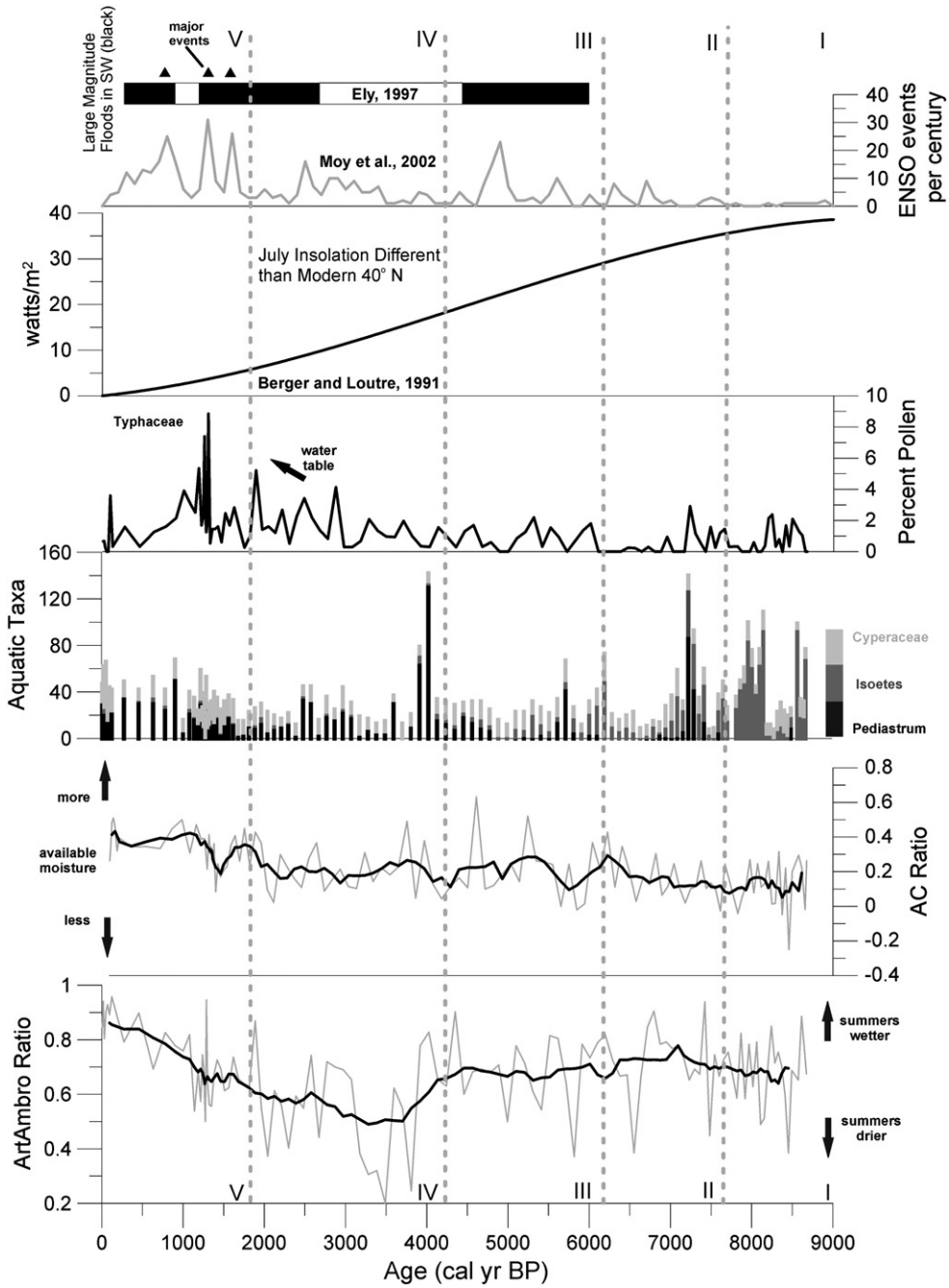

Figure 5. Terrestrial pollen ratios and aquatic-type taxa from Morris Pond depicting vegetation change and moisture trends over the last 8600 cal yr BP. ENSO (Moy et al., 2002), summer insolation data (Berger and Loutre, 1991), and paleoflood chronology from the Virgin River drainage (Ely, 1997) are also depicted. Dashed vertical lines indicate fire regime zone derived from regime shift index algorithm (RSI) (Rodionov, 2004).

Aquatic taxa are less abundant in Zone III than in Zones I and II and are composed of *Isoetes* and Cyperaceae. *Pediastrum* rises briefly at ca. 5800 cal yr BP. Typhaceae is low (≤2%) (Fig. 5).

Charcoal

Zone III BCHAR averages 0.02 cm^2/yr and FRI averages 679 yr (Fig. 4). This period represents the lowest amount of BCHAR and highest FRI of the five zones. Three discrete charcoal peaks occur. Peak magnitudes range between 0.3 and 2.1 and average 1.4 particles/peak.

Zone IV: 4200–1800 cal yr BP

Pollen

Zone IV assemblage includes the lowest average AP of the five zones (47%) with abundant shrubs (31%) and herbs (22%). *Picea* pollen averages are the greatest component of AP (23%) while *Pinus* is also important (19%) (Fig. 3). *Abies* and *Populus* are variable (2–4%). *Pseudotsuga* is highest of the five zones during this period. Predominant shrubs include *Artemisia* (14%), Chenopodiaceae (7%), and Rosaceae (3%). *Ambrosia* and Ephedraceae occur in the greatest amount of the record (6–7% and 2%, respectively). Herbs are dominated by Poaceae (11%) and Asteraceae (4%). Total pollen influx averages 3565 grains/cm^2/yr (Fig. 4). Aquatic taxa are less abundant in Zone IV than in Zone II and Zone I and are primarily composed of *Isoetes* and Cyperaceae. *Pediastrum* peaks at ca. 3800 cal yr BP (140 spores) and then decreases over the remaining record (≤20 spores/cm^2/yr). Typhaceae pollen increases and is variable (2–6%) (Fig. 5).

Charcoal

Zone IV BCHAR averages 0.06 cm^2/yr and FRI averages 270 yr (Fig. 4). Twelve discrete charcoal peaks occur and represent the greatest number of peaks in any zone over the record. Peak magnitude ranges between 0.1 and 47.5 and averages 5.8 particles/peak.

Zone V: 1800 cal yr BP–modern

Pollen

Zone V assemblage includes the most abundant average AP (57%) of the record while subalpine shrubs (24%) and herbs (19%) are lower than previous zones. *Picea* is highest of the record (29%). *Pinus* is also important (18%) and *Abies* increases to 7% while *Populus* averages 2% (Fig. 3). AP exhibits conspicuous fluctuations at ca. 1200 cal yr BP. *Pseudotsuga* declines and becomes nearly absent in Zone V. Shrubs include *Artemisia* (18%), Chenopodiaceae (5%), and Rosaceae (3%). *Ambrosia* decreases to 2% while Ephedraceae maintains 2%. Herbs include Poaceae (11%) and Asteraceae (5%). Poaceae pollen peaks at 1200 cal yr BP (20%). Total pollen influx averages 7583 grains/cm^2/yr and is the highest average influx of the record (Fig. 4). The aquatic assemblage is dominated by Cyperaceae and *Pediastrum* which generally increase towards modern. Typhaceae pollen is elevated and fluctuates at ca. 1200 cal yr BP (Fig. 5).

Charcoal

Zone V BCHAR averages 0.2 cm^2/yr and FRI averages 351 yr (Fig. 4). Six discrete charcoal peaks occur. Peak magnitude ranges between 0.5 and 47.1 and averages 9 particles/peak.

Discussion

Zone I: 8600–7700 cal yr BP

MP began accumulating sediment at ca. 8600 cal yr BP, which is consistent with other subalpine lakes on the Colorado Plateau (Shafer, 1989; Morris, 2011). Beginning at ca. 9000 cal yr BP, Anderson (2011, 2012) suggests that a greater proportion of precipitation arrived as snow relative to rain in eastern highlands of the Colorado Plateau. Because winter snowfall is known to be an important control on lake level (Shuman et al., 2009), we suggest that increasing snowpack in this zone resulted in perennially wet conditions at MP.

Palynological and paleobotanical data, including this record, indicate that early Holocene summers on the Markagunt were both warm and wet (Anderson et al., 1999; Mock and Brunelle-Daines, 1999; Madsen et al., 2002). The NAM expanded northward and increased in intensity during the early Holocene (Bartlein et al., 1998). In Zone I, the AP assemblage is dominated by *Picea* and *Pinus* and total pollen influx is high within the context of the record, suggesting abundant woody biomass (Fig. 3, Table 2). The Zone I fire regime is characterized by high magnitude peaks, with the greatest average BCHAR of the five zones (Fig. 4; Table 2). Charcoal data also suggest that available biomass would burn when conditions were favorable. High *Pinus* pollen, probably *P. flexilis*, indicates that fires consumed biomass sufficiently to expose mineral soil because *P. flexilis* establishment is high in subalpine forests following fires where mineral soil is exposed (Peet, 1981). The high frequency of fire as indicated by a FRI of 178 yr in Zone I would maintain forests dominated by *P. flexilis* over *Picea engelmannii* (Peet, 1981).

In general, forests in the southwest are at greater risk for fire during La Niña episodes and negative-phase PDO (Schoennagel et al., 2005; Brown et al., 2008). Four charcoal peaks cluster at ca. 8200 cal yr BP (Fig. 4) and decreases in aquatic taxa suggest that winter aridity prevailed, possibly due to a temporary hiatus in snow delivery from persistent La Niña-like conditions (Fig. 5) (Moy et al., 2002). Modern studies suggest that low snowfall years in the Colorado Plateau yield subsequent NAM enhancements due to increased land/sea temperature contrasts (Notaro and Zarrin, 2011). At 8200 cal yr BP, the glacial anticyclone over the collapsing Laurentide Ice Sheet weakened and the westerly Pacific storm track shifted, resulting in dramatic climate variability in the northern hemisphere (Alley and Ágústsdóttir, 2005). At Red Valley Bog, a hiatus in sediment deposition at 8200 cal yr BP suggests that winter aridity and/or variable hydrologic conditions occurred on the Markagunt (Madsen et al., 2002). Compared to other zones, *Picea* pollen accumulations are low at MP and LCB (Fig. 3). Anderson et al. (1999) offer several possible explanations for reduced *Picea* pollen, including a potential *D. rufipennis* disturbance. Our record suggests that variability in *Picea* pollen noted by Anderson et al. (1999) may reflect frequent fire disturbances in the Lowder Creek drainage (Fig. 4). The results from MP cannot specifically diagnose (or eliminate) a *D. rufipennis* epidemic because no insect macrofossils were recovered (e.g., Brunelle et al., 2008), although the MP record suggests that fire disturbance was prominent at 8200 cal yr BP. The early Holocene climate supported greater fire frequency because reduced winter snowpack from pervasive La Niña conditions increased the length of fire season and an enhanced NAM that resulted in greater occurrence of convective storms and lightning.

Zone II: 7700–6200 cal yr BP

Growing season conditions during Zone II were warm and wet. Madsen et al. (2002) and Reinemann et al. (2009) found that middle Holocene temperatures in the region were similar to or slightly warmer than modern. Model simulations suggest abundant moisture, intense surface heating, and 1–2°C (Braconnot et al., 2007) or 3–5°C (Renssen et al., 2012) summer temperature increases. The NAM continued to supply ample growing season precipitation and intense surface heating enhanced lower atmosphere convection, and lightning activity (Diffenbaugh et al., 2006). Fall (1997) suggests that NAM precipitation facilitated a downslope migration of lower timberline in western Colorado while warm growing season temperatures were favorable for a simultaneous upslope advance.

The MP pollen record indicates that *Picea* and *Pinus* were predominant forest components in Zone II and low shrub pollen suggests closed-canopy forests conditions (Fig. 3; Table 2). The fire regime is unique because it is dominated by three large-magnitude peaks, greatly exceeding values found in other zones, which is indicative of closed-canopy forest

conditions (Table 2). The co-occurrence of magnetic susceptibility peaks and charcoal peaks (Fig. 4) suggests that fire episodes resulted in either substantial erosion events or conversion of soil to ferromagnetic minerals (or both) (e.g., Gedye et al., 2000). In no other zone is there similar correspondence between the MS and charcoal profiles. The reciprocal exchange of *Picea* and *Pinus* pollen in Zone II (e.g., Fig. 3a at 7600 cal yr BP) is probably related to changes in stand and recruitment dynamics following stand-replacing fire events.

Zone III: 6200–4200 cal yr BP

Zone III reflects a trend from mesic towards xeric growing-season conditions, probably resulting from declining summer insolation and corresponding retraction of the NAM (Diffenbaugh et al., 2006; Anderson, 2012). The MP *Artemisia*/*Ambrosia* ratio indicates only a slight decline in growing-season moisture, although this trend decreases throughout Zone III (Fig. 5). Anderson et al. (1999) propose that moisture deficits prevailed at this time and that stand density decreased around LCB. The MP record supports an interpretation of increased aridity (Figs. 3 and 5). BCHAR, total pollen influx, AP, and shrub pollen are low within the context of the record (Fig. 4; Table 2) suggesting that biomass and fuel connectivity were probably greatly reduced in Zone III compared to Zones I and II.

Increases of *Pseudotsuga* pollen near the end of Zone III provide evidence of drier growing season conditions at MP (Fig. 3). The establishment of *Pseudotsuga* is generally interpreted as evidence of persistent aridity because *Pseudotsuga* prefers seasonal dryness (Thompson et al., 1999). Concurrent with increases at MP, *Pseudotsuga* pollen also increased at Red Valley Bog, Aquarius Plateau, and Kaibab Plateau (Weng and Jackson, 1999; Madsen et al., 2002; Morris, 2011). Weng and Jackson (1999) also interpret this period as having dry summer conditions. Fall (1997) suggests that lower timberline retreated upslope from a retracted NAM in western Colorado. At MP *Polygonum*, a mesophytic herb disappears in Zone III. Mock and Brunelle-Daines (1999) note that lake levels were essentially unchanged from modern at this time, which indicates that surface water is probably insensitive to changes in summer moisture conditions and supports an interpretation that lake level reflects snowpack conditions (Shuman et al., 2009). Reinemann et al. (2009) found that 5400 cal yr BP was a time of peak warmth during the middle Holocene in the central Great Basin. The MP record suggests that this period was warm and dry, but we cannot specifically address whether or not peak temperature occurred in the eastern margin of the Great Basin at this time. The MP charcoal record indicates that biomass burning was lowest during this period. A reduction in biomass burning could occur during peak warmth if warm conditions were concomitant with substantial growing-season moisture deficits. Peak warmth and subdued NAM contrasts conditions on the Markagunt during the early Holocene, but climate model simulations suggest that increased subsidence (i.e., high pressure) occurred over the Colorado Plateau during the mid-Holocene, which could account for the dry conditions at MP (Zhao and Harrison, 2011).

The fire regime in Zone III contrasts those of Zones I and II in that BCHAR and RSI are lower. This decrease probably reflects a transition to a fuel-limited fire regime and reduced length of fire season from increasing snow cover (Fig. 5). Drier growing-season conditions probably favored lower conifer recruitment (Fig. 3). FRI are the longest of the five zones (679 yr). Total pollen influx and BCHAR are the lowest of the record (Fig. 4), supporting an interpretation of reduced biomass and connectivity of woody forest fuels in comparison to Zones I and II. Ely (1997) notes numerous large magnitude flood events in the Virgin River drainage, which has its headwaters on the Markagunt (Fig. 5). Sparse vegetative cover is known to be an important contributor to flooding episodes in this region (Hall, 2001; Harden et al., 2010). Also at this time, Moy et al. (2002) and Conroy et al. (2008) suggest that ENSO intensity and frequency increased (Fig. 5). It is possible that when coupled with sparse vegetative cover, melting of significant accumulations of winter snowpack and cold season climate conditions could be important for paleofloods in this region (Harden et al., 2010). It is interesting to note that flood-induced erosion events are not detected in the MS profile, suggesting that ferromagnetic enhancements in the sedimentary profile are mainly related to intense heating during fire events, such as those evident in Zone II (Gedye et al., 2000).

Zone IV: 4200–1800 cal yr BP

Summers in Zone IV continued to cool from reduced summer insolation (Fig. 5; Berger and Loutre, 1991) and intensity of the NAM and convective precipitation events continued to decline (Shafer, 1989; Bartlein et al., 1998; Madsen et al., 2002). In eastern Nevada, chironomid-inferred summer temperatures suggest pervasive cooling between 4000 and 2000 cal yr BP (Reinemann et al., 2009). *Artemisia*/*Ambrosia* ratios from MP and two lakes on the Aquarius Plateau (Shafer, 1989; Morris, 2011) suggest arid growing-season conditions (Fig. 5). This period at MP exhibits the highest average shrub pollen (40%) suggesting an opening forest canopy with a well-developed shrub understory. *Pseudotsuga* pollen persists throughout this period, also supporting inferences of summer aridity.

In contrast to xeric growing-season conditions, winter precipitation was likely increasing. Moy et al. (2002) and Conroy et al. (2008) infer that an intensification of ENSO beginning around 4200 cal yr BP would have contributed to greater winter precipitation in the southwest. Anderson (2011, 2012) notes a step-wise transition of increasing snowfall relative to rain at 3000 cal yr BP. In Zone IV, *Abies* pollen (presumably *Abies lasiocarpa*) becomes more abundant, consistent with regional pollen records (Fall, 1997; Feiler et al., 1997; Anderson et al., 1999; Weng and Jackson, 1999; Morris, 2011). Fall (1997) notes that *A. lasiocarpa* thrives in deep and persistent winter snowpack, supporting our interpretation that cold-season precipitation as snowfall generally increased during the late Holocene at MP. *A. lasiocarpa* is also shade-tolerant and successfully establishes in the absence of fire and in forest or shrub understory.

Beginning at ca. 4500 cal yr BP, a decreasing trend in *Pinus* pollen occurs at MP and LCB (Fig. 3) (Anderson et al., 1999). Declining *Pinus* pollen could be related to recruitment exclusion from an absence of fires that exposed mineral soil. In contrast to *A. lasiocarpa*, *P. flexilis* requires full light exposure to germinate and is shade-intolerant (Peet, 1981). Shrub influx is high and therefore could have inhibited *P. flexilis* establishment. The modest increase in total pollen influx reflects increases in subalpine shrub pollen. Fire episodes are frequent and of low magnitude, suggesting that low-intensity fires in shrubs were probably typical, though these burning events did not consume substantial woody biomass, evolve to stand-replacing episodes, and/or alter the ferromagnetic properties of the soil as did the peak episodes in Zones I and II.

Zone V: 1800 cal yr BP–modern

Lake levels across the southern Colorado Plateau generally increased during the late Holocene (Fig. 5) (Anderson et al., 1999; Weng and Jackson, 1999). *Abies* continues to increase in importance at MP (Fig. 3) and elsewhere in the region (e.g., Fall, 1997; Morris et al., 2010; Morris, 2011). Increasing frequency of ENSO (Fig. 5) (Moy et al., 2002), coupled with a continuation of decreasing summer insolation (Fig. 5) (Berger and Loutre, 1991) suggests generally cool and wet conditions, and a continued trend of increasing snow relative to rain (Anderson, 2011, 2012). The increase in Typhaceae pollen that begins near the end of Zone IV and continues into Zone V suggests local paludification from a rising water table (Fig. 5). Typhaceae prefers moist, hummocky conditions and we interpret the increase in abundance of Typhaceae pollen to be indicative of increasingly mesic conditions brought on by greater snow delivery during the late Holocene relative to the middle and early Holocene.

At 1200 cal yr BP, the Morris Pond pollen record suggests variable moisture conditions, probably related in part to high ENSO variability (Figs. 3 and 5). Tree-ring chronologies from the Tavaputs Plateau indicate several large-amplitude pluvial/drought oscillations between 1250 and 1050 cal yr BP (Knight et al., 2010). Conspicuous increases in moisture-sensitive taxa (Fig. 5) and high pollen influx (Fig. 4) suggest significant variability in both summer and winter precipitation. The fire regime is unique in that fire is infrequent with low peak magnitudes. Increasing summer temperatures in the central Great Basin (Reinemann et al., 2009) and high AP and total pollen influx at MP suggest that summer and fuel conditions were otherwise conducive to frequent high-intensity burning during the late Holocene. However, the MP record suggests that the increasing importance and persistence of snowpack during the late Holocene dominates the fire regime in Zone V, causing it to be fuel-abundant and climate-limited. This claim is supported by stand reconstructions of late Holocene fire disturbance on the Markagunt (DeRose and Long, 2012).

Over the last millennia, the fire regime at MP has been similar to Zone IV in terms of FRI, though peak magnitudes are not as large. BCHAR is most similar to Zone I. Over the last 1000 yr AP is generally more abundant than NAP, though highly variable (Fig. 4). Based on pollen influx evidence, a warming 21st century yielding longer snow-free periods (Westerling et al., 2006) may shift fire regimes on the southern Markagunt Plateau towards larger magnitude events, perhaps similar to Zones I and II in our reconstruction. Further examination of Zone V paired with tree-ring reconstructions could provide greater insight.

Conclusions

The composition of the vegetation community on the Markagunt Plateau has changed modestly over the last 8600 cal yr BP. Pollen data suggest that the subalpine forest zone of the Markagunt has been dominated by *Picea*, with variable *Abies* and *Pinus* components. In contrast, the reconstructed fire regime exhibits considerable variability over this same time period. Evidence from this reconstruction suggests that millennial-scale fire regimes are strongly influenced by climate-mediated forest structure, fuel connectivity, and available biomass. Precipitation seasonality, length of snow-free period, and seasonal temperature are important controls on fire occurrence whose dynamics over the Holocene have been dominated by insolation-driven changes to the climate system, specifically NAM and ENSO.

We defined the statistically significant shifts in the fire regime by applying a regime shift index (Rodionov, 2004) to BCHAR (Higuera et al., 2009) and show that significant regime shifts occurred at 7700, 6200, 4200, and 1800 cal yr BP. The role of millennial-scale climate forcing in shaping wildfire regimes on the Markagunt is important and yields a wide array of fire frequencies and inferred peak magnitudes. While the structure of the vegetation community appears to be important (trees relative to shrubs), the forest composition is likely an artifact of fire disturbance (or lack thereof) rather than a causal mechanism (e.g., Zones I and II vs. IV and V for *Pinus*).

The high-resolution pollen and charcoal record from MP generally agrees with other paleoenvironmental reconstructions in the southwestern USA. Between 8600 and 6200 cal yr BP the climate can be characterized by greater amounts of summer precipitation and less winter precipitation than at present. The fire regime from 8600 to 7700 cal yr BP was fuel-abundant with frequent, large magnitude burning episodes. The period between 7700 and 6200 cal yr BP was unique because of the anomalously large peak-magnitude burning episodes (inferred from charcoal and MS), when high-intensity crown fires likely prevailed on the Markagunt. Ample forest fuels and warm temperatures allowed substantial biomass burning and persistent La Niña conditions lengthened fire season, therefore allowing greater opportunities for large conflagrations to occur. At 6200 cal yr BP the fire regime transitioned from a fuel abundant to a fuel limited system. From 1800 cal yr BP to modern times, the fire regime is climate-limited due to prevailing cool and wet conditions and decreased length of the snow-free period. During the 21st century, warmer summers and increased length of fire season may lead to a fire regime on the Markagunt Plateau similar to that occurred from 7700 to 6200 cal yr BP or 8600 to 6200 cal yr BP.

Acknowledgments

Support for this research was provided by a Doctoral Dissertation Research Improvement Grant from the National Science Foundation to JM (1032099) and from an award from the Joint Fire Science Program to AB (063131). We extend our gratitude to Stacy Morris, Tyler Morris, and Todd Daines for assistance with sediment retrieval and to A. Steven Munson, Lesleigh Anderson, and Rosemary Sherriff for theoretical contributions during field work. We thank Douglas Dvoracek at CAIS for AMS consultation and James Budahn at USGS Denver for $^{210}Pb/^{137}Cs$ analysis. We are grateful to Ken Adams and two anonymous reviewers whose comments and suggestions greatly improved our manuscript.

References

Adams, D.K., Comrie, A.C., 1997. The North American Monsoon. Bulletin of the American Meteorological Society 78, 2197–2213.
Ali, A.A., Higuera, P.E., Bergeron, Y., Carcaillet, C., 2009. Comparing fire-history interpretations based on area, number and estimated volume of macroscopic charcoal in lake sediments. Quaternary Research 72, 462–486.
Alley, R.B., Ágústsdóttir, A.M., 2005. The 8k event: cause and consequences of a major Holocene abrupt climate change. Quaternary Science Reviews 24, 1123–1149.
Anderson, L.A., 2011. Holocene record of precipitation seasonality from lake calcite $\delta^{18}O$ in the central Rocky Mountains, United States. Geology 39, 211–214.
Anderson, L.A., 2012. Rocky Mountain hydroclimate: Holocene variability and the role of insolation, ENSO, and the North American Monsoon. Global and Planetary Change 92–93, 198–208.
Anderson, R.S., Hasbargen, J., Koehler, P.A., Feiler, E.J., 1999. Late Wisconsin and Holocene subalpine forests of the Markagunt Plateau of Utah, southwest Colorado Plateau, USA. Arctic, Antarctic, and Alpine Research 31, 366–378.
Anderson, R.S., Betancourt, J.L., Mead, J.I., Hevly, R.H., Adam, D.P., 2000. Middle- and late-Wisconsin paleobotanic and paleoclimatic records from the southern Colorado Plateau, USA. Palaeogeography, Palaeoclimatology, Palaeoecology 155, 31–57.
Appleby, P.G., Oldfield, F., Thompson, R., Huttunen, P., Tolonen, K., 1979. ^{210}Pb dating of annually laminated lake sediments from Finland. Nature 280, 53–55.
Arno, S.F., Hammerly, R.P., 1984. Timberline: Mountain and Arctic Forest Frontiers. The Mountaineers, Seattle.
Bartlein, P.J., Anderson, K.H., Anderson, P.M., Edwards, M.E., Mock, C.J., Thompson, R.S., Webb, R.S., Webb III, T., Whitlock, C., 1998. Paleoclimate simulations for North America over the past 21,000 years: features of the simulated climate and comparisons with paleoenvironmental data. Quaternary Science Reviews 17, 549–585.
Bassett, I.J., Crompton, C.W., Parmlee, J.A., 1978. An Atlas of Airborne Pollen Grains and Common Fungal Spores. Biosystematics Research Institute, Ottawa.
Bennett, K.D., 1996. Determination of the number of zones in a biostratigraphical sequence. New Phytologist 132, 155–170.
Berger, A., Loutre, M.F., 1991. Insolation values for the climate of the last 10 million years. Quaternary Science Reviews 10, 297–317.
Biondi, F., Gershunov, A., Cayan, D., 2001. North Pacific decadal climate variability since 1661. Journal of Climate 14, 5–10.
Braconnot, P., Otto-Bliesner, B., Harrison, S., Joussaume, S., Peterchmitt, J.-Y., Abe-Ouchi, A., Crucifix, M., Driesschaert, E., Fichefet, T., Hewitt, C.D., Kageyama, M., Kitoh, A., Laıne, A., Loutre, M.F., Marti, O., Merkel, U., Ramstein, G., Valdes, P., Weber, S.L., Yu, Y., Zhao, Y., 2007. Results of PMIP2 coupled simulations of the Mid-Holocene and Last Glacial Maximum — parts 1 and 2: experiments and large-scale features. Feedbacks with emphasis on the location of the ITCZ and mid- and high latitudes heat budget. Climate of the Past 3, 261–296.
Brown, P.M., Heyerdahl, E.K., Kitchen, S.G., Weber, M.H., 2008. Climate effects on historical fires (1630–1900) in Utah. International Journal of Wildland Fire 17, 28–39.
Brunelle, A.R., Rehfeldt, J., Bentz, B.J., Munson, A.S., 2008. Holocene records of mountain pine beetle infestation in the U.S. Northern Rocky Mountains. Forest Ecology and Management 255, 836–846.
Cable, D.R., 1977. Soil water changes in the creosote bush and bursage during a dry period in southern Arizona. Journal of the Arizona Academy of Science 12, 15–20.
Clark, J.S., 1988. Particle motion and the theory of charcoal analysis: source area, transport, deposition, and sampling. Quaternary Research 30, 67–80.
Conedera, M., Tinner, W., Neff, C., Meurer, M., Dickens, A.F., Kerbs, P., 2009. Reconstructing past fire regimes: methods, applications, and relevance to fire management and conservation. Quaternary Science Reviews 28, 555–576.
Conroy, J.L., Overpeck, J.T., Cole, J.E., Shanahan, T.M., Steinitz-Kannan, M., 2008. Holocene changes in eastern tropical Pacific climate inferred from a Galápagos lake sediment record. Quaternary Science Reviews 27, 1166–1180.
Davis, O.K., 1990. Caves as sources of biotic remains in arid western North America. Palaeogeography, Palaeoclimatology, Palaeoecology 76, 331–348.

Davis, O.K., Pitblado, B.L., 1995. Late glacial aridity in the Southern Rocky Mountains. In: Waugh, W.J., Petersen, K.L., Wigand, P.E., Louthan, B.D., Walker, R.D. (Eds.), Climate Change in the Four Corners and Adjacent Regions: Implications for Environmental Restoration and Land-use Planning. USDOE: CONF-9409325, Springfield, pp. 9–23.
Dean, W.E., 1974. Determination of carbonate and organic matter in calcerous sediments by loss on ignition comparison to other methods. Journal of Sedimentary Petrology 44, 242–248.
DeRose, R.J., Long, J.N., 2007. Disturbance, structure, and composition: spruce beetle and Engelmann spruce forests on the Markagunt Plateau, Utah. Forest Ecology and Management 244, 16–23.
DeRose, R.J., Long, J.N., 2012. Drought driven disturbance history characterizes a southern Rocky Mountain subalpine forest. Canadian Journal of Forest Research 42, 1649–1660.
Diffenbaugh, N.S., Ashfaq, M., Shuman, B., Williams, J.W., Bartlein, P.J., 2006. Summer aridity in the United States: response to mid-Holocene changes in insolation and sea surface temperature. Geophysical Research Letters 33 http://dx.doi.org/10.1029/2006GL028012.
Ely, L., 1997. Response of extreme floods in the southwestern United States to climatic variations in the late Holocene. Geomorphology 19, 175–201.
Erdtman, G., 1952. Pollen Morphology and Plant Taxonomy: Angiosperms. Almqvist and Wiksell, Stockholm.
Fægri, K., Kaland, P.E., Kzywinski, K., 1989. Textbook of Pollen Analysis. John Wiley and Sons, New York.
Falk, D.A., Swetnam, T.W., 2003. Scaling rules and probability models for surface fire regimes in ponderosa pine forests. USDA Forest Service Proceedings RMRSP 29, 301–318.
Fall, P.L., 1997. Timberline fluctuations and late Quaternary paleoclimates in the southern Rocky Mountains, Colorado. Geological Society of America Bulletin 109, 1306–1320.
Feiler, E.J., Anderson, R.S., Koehler, P.A., 1997. Late Quaternary paleoenvironments of the White River Plateau, Colorado, USA. Arctic and Alpine Research 29, 53–62.
Ford, D.C., Williams, P.W., 2007. Karst Geomorphology and Hydrology. John Wiley and Sons, New York.
Gardner, J.J., Whitlock, C., 2001. Charcoal accumulation following a recent fire in the Cascade Range, northwestern USA, and its relevance for fire-history studies. The Holocene 11, 541–549.
Gavin, D.G., Hu, F.S., Lertzman, K., Corbett, P., 2006. Weak climatic control of stand-scale fire history during the Late Holocene in southeastern British Columbia. Ecology 87, 1722–1732.
Gedye, S.J., Jones, R.T., Tinner, W., Ammann, B., Oldfield, F., 2000. The use of mineral magnetisms in the reconstruction of fire history: a case study from Lago di Origlio, Swiss Alps. Palaeogeography, Palaeoclimatology, Palaeoecology 164, 101–110.
Goldstrand, P.M., 1994. Tectonic development of Upper Cretaceous to Eocene strata of southwestern Utah. Geological Society of America Bulletin 106, 145–154.
Gregory, H.E., 1949. Geologic and geographic reconnaissance of eastern Markagunt Plateau, Utah. Geological Society of America Bulletin 60, 969–997.
Grimm, E.C., 1987. CONNISS: a FORTRAN 77 programme for stratigraphically constrained cluster analysis by the method of incremental sum of squares. Computers and Geoscience 13, 13–35.
Hall, M., 2001. Repairing mountains: restoration, ecology and wilderness in twentieth-century Utah. Environmental History 6, 574–600.
Harden, T., Macklin, M.G., Baker, V.R., 2010. Holocene flood histories in south-western USA. Earth Surface Processes and Landforms 35, 707–716.
Herzschuh, U., 2007. Reliability of pollen ratios for environmental reconstructions on the Tibetan Plateau. Journal of Biogeography 34, 1265–1273.
Higuera, P.E., Whitlock, C., Gage, J.A., 2011. Linking tree-ring and sediment-charcoal records to reconstruct fire occurrence and area burned in subalpine forests of Yellowstone National Park, USA. The Holocene 21 http://dx.doi.org/10.1177/0959683610374882.
Higuera, P.E., Peters, M.E., Brubaker, L.B., Gavin, D.G., 2007. Understanding the origin and analysis of sediment-charcoal records with a simulation model. Quaternary Science Reviews 26, 1790–1809.
Higuera, P.E., Brubaker, L.B., Anderson, P.M., Hu, F.S., Brown, T.A., 2009. Vegetation mediated the impacts of postglacial climatic change on fire regimes in the south-central Brooks Range, Alaska. Ecological Monographs 79, 201–219.
Higuera, P.E., Gavin, D.G., Bartlein, P.J., Hallett, D.J., 2010. Peak detection in sediment-charcoal records: impacts of alternative data analysis methods on fire-history interpretations. International Journal of Wildland Fire 19, 996–1014.
Kapp, R.O., Davis, O.K., King, J.E., 2000. Pollen and Spores, 2nd ed. American Association of Stratigraphic Palynologists, New York.
Knight, T.A., Meko, D.M., Baisan, C.H., 2010. A bimillennial-length tree-ring reconstruction of precipitation for the Tavaputs Plateau, northeastern Utah. Quaternary Research http://dx.doi.org/10.1016/j.yqres.2009.08.002.
Long, C.J., Whitlock, C., Bartlein, P.J., Millspaugh, S.H., 1998. A 9000-year fire history from the Oregon Coast Range, based on a high-resolution charcoal study. Canadian Journal of Forest Research 28, 774–787.
Lundeen, Z., 2012. Paleoecological and Isotopic Records of Climate Change and Variability, Bear River Range, Southeast Idaho. Ph.D. Dissertation, University of Utah.
Lynch, J.A., Hollis, J.L., Hu, F.S., 2004. Climatic and landscape controls of the boreal fire regime: Holocene records from Alaska. Journal of Ecology 92, 477–489.
Madsen, D.B., Elias, S.A., Weng, C., Jackson, S.T., Thompson, R.S., Rhode, D., 2002. The Paleoecology of Red Valley Bog, Markagunt Plateau, Utah. Utah Geological Survey Technical Report.
Maher, L.J., 1963. Pollen analyses of surface materials from the southern San Juan Mountains, Colorado. GSA Bulletin 74, 1485–1504.
Mantua, N.J., Hare, S.R., Zhang, Y., Wallace, J.M., Francis, R.C., 1997. A Pacific interdecadal oscillation with impacts on salmon production. Bulletin of the American Meteorological Society 78, 1069–1079.
Marlon, J., Bartlein, P.J., Whitlock, C., 2006. Fire–fuel–climate linkages in the northwestern USA during the Holocene. The Holocene 16, 1059–1071.
Marlon, J.R., Bartlein, P.J., Carcaillet, C., Gavin, D.G., Harrison, S.P., Higuera, P.E., Joos, F., Power, M.J., Prentice, I.C., 2008. Climate and human influences on global biomass burning over the past two millennia. Nature Geoscience http://dx.doi.org/10.1038/ngeo313.
McCabe, G.J., Dettinger, M.D., 1999. Decadal variations in the strength of ENSO teleconnections with precipitation in the western United States. International Journal of Climatology 19, 1399–1410.
Mensing, S.A., Benson, L.V., Kashgarian, M., Lund, S., 2004. A Holocene pollen record of persistent droughts from Pyramid Lake, Nevada, USA. Quaternary Research 62, 29–38.
Mock, C.J., 1996. Climate controls and spatial variations of precipitation in the western United States. Journal of Climate 9, 1111–1125.
Mock, C.J., Brunelle-Daines, A., 1999. A modern analogue of western United States summer paleoclimate at 6000 years before present. The Holocene 9, 541–545.
Morris, J.L., 2011. Historic and Holocene forest disturbance in south central Utah. Ph.D. Dissertation, University of Utah.
Morris, J.L., Brunelle, A., 2012. Pollen records of historic spruce beetle (*Dendroctonus rufipennis*) disturbance from the subalpine ranges of southern Utah, USA. The Holocene http://dx.doi.org/10.1177/0959683612437870.
Morris, J.L., Brunelle, A., Munson, A.S., 2010. Pollen evidence of historical forest disturbance on the Wasatch Plateau, Utah. Western North American Naturalist 70, 175–188.
Moy, C.M., Selzer, G.O., Rodbell, D.T., Anderson, D.M., 2002. Variability of El Niño/Southern Oscillation activity at millennial timescales during the Holocene epoch. Nature 420, 162–165.
Mulvey, W.E., Currey, D.R., Lindsay, L.M.W., 1984. Southernmost occurrence of later Pleistocene glaciation in Utah: Brian Head-Sidney Peaks area, Markagunt Plateau. Encyclia 61, 97–101.
Notaro, M., Zarrin, A., 2011. Sensitivity of the North American monsoon to antecedent Rocky Mountain snowpack. Geophysical Research Letters 38 http://dx.doi.org/10.1029/2011GL048803.
Ohlson, M., Brown, K.J., Birks, H.J.B., Grytnes, J.A., Hörnberg, G., Niklasson, M., Seppä, H., Bradshaw, R.H.W., 2011. Invasion of Norway spruce diversifies the fire regime in European forests. Journal of Ecology 99, 395–403.
Peet, R.K., 1981. Forest vegetation of the Colorado Front Range: composition and dynamics. Vegetatio 45, 3–75.
Power, M.J., 84 co authors, 2008. Changes in fire regime since the Last Glacial Maximum: an assessment based on a global synthesis and analysis of charcoal data. Climate Dynamics 30, 887–907.
Power, M.J., Marlon, J.R., Bartlein, P.J., Harrison, S., 2010. Fire history and the global charcoal database: a new tool for hypothesis testing and data exploration. Palaeogeography, Palaeoclimatology, Palaeoecology 291, 52–59.
Power, M.J., Mayle, F.E., Bartlein, P.J., Marlon, J.R., Anderson, R.S., Behling, H., Brown, K.J., Carcaillet, C., Colomboroli, D., Gavin, D.G., Hallett, D.J., Horn, S.P., Kennedy, L.M., Lane, C.S., Long, C.J., Moreno, P.I., Paitre, C., Robinson, G., Taylor, Z., Walsh, M.K., 2012. Climatic control of the biomass-burning decline in the Americas after A.D. The Holocene 1500 http://dx.doi.org/10.1177/0959683612450196.
Raffa, K.F., Aukema, B.H., Bentz, B.J., Carroll, A.L., Hicke, J.A., Turner, M.G., Romme, W.H., 2008. Cross-scale drivers of natural disturbances prone to anthropogenic amplification: the dynamics of bark beetle eruptions. Bioscience 58, 501–517.
Reimer, P.J., Baillie, M.G.L., Bard, E., Bayliss, A., Beck, J.W., Bertrand, C., Blackwell, P.G., Buck, C.E., Burr, G., Cutler, K.B., Damon, P.E., Edwards, R.L., Fairbanks, R.G., Friedrich, M., Guilderson, T.P., Hughen, K.A., Kromer, B., McCormac, F.G., Manning, S., Bronk Ramsey, C., Reimer, R.W., Remmele, S., Southon, J.R., Stuiver, M., Talamo, S., Taylor, F.W., van der Plicht, J., Weyhenmeyer, C.E., 2009. Intcal09 and Marine09 radiocarbon age calibration curves, 0–50,000 years cal BP. Radiocarbon 51, 1111–1150.
Reinemann, S.A., Porinchu, D.F., Bloom, A.M., Mark, B.G., Box, J.E., 2009. A multi-proxy paleolimnological reconstruction of Holocene climate conditions in the Great Basin, USA. Quaternary Research 72, 347–358.
Renssen, H., Seppä, H., Crosta, X., Goosse, H., Roche, D.M., 2012. Global characterization of the Holocene Thermal Maximum. Quaternary Science Reviews 48, 7–19.
Ritchie, J.C., 1995. Current trends in studies of long-term plant community dynamics. New Phytologist 130, 469–494.
Rodionov, S.N., 2004. A sequential algorithm for testing climate regime shifts. Geophysical Research Letters 31, L09204 http://dx.doi.org/10.1029/2004GL019448.
Ropelewski, C.F., Halpert, M.S., 1986. North American precipitation and temperature patterns associated with the El Niño/Southern Oscillation (ENSO). Monthly Weather Reviews 114, 2352–2362.
Scheffer, M., Carpenter, S., Foley, J.A., Folkes, C., Walker, B., 2001. Catastrophic shifts in ecosystems. Nature 413, 591–596.
Schoennagel, T., Veblen, T.T., Romme, W.H., Sibold, J.S., Cooke, E.R., 2005. ENSO and PDO variability affect drought-induced fire occurrence in Rocky Mountain subalpine forests. Ecological Applications 15, 2000–2014.
Seppä, H., Alenius, T., Muukkonen, P., Giesecke, T., Miller, P.A., Ojala, A.E.K., 2009. Calibrated pollen accumulation rates as a basis for quantitative tree biomass reconstructions. The Holocene 19, 209–220.
Shafer, D.S., 1989. The timing of late Quaternary monsoon precipitation maxima in the southwest United States. Ph.D. Dissertation, University of Arizona.
Shuman, B., Henderson, A.K., Colman, S.M., Stone, J.R., Fritz, S.C., Stevens, L.R., Power, M.J., Whitlock, C., 2009. Holocene lake-level trends in the Rocky Mountains, U.S.A. Quaternary Science Reviews 28, 1861–1879.
Thompson, R.S., Anderson, K.H., Bartlein, P.J., 1999. Atlas of relations between climatic parameters and distributions of important trees and shrubs in North America. USGS Professional Papers 1650a,b.

Weng, C., Jackson, S.T., 1999. Late Glacial and Holocene vegetation history and paleoclimate of the Kaibab Plateau, Arizona. Palaeogeography, Palaeoclimatology, Palaeoecology 153, 179–201.
Westerling, A.L., Hidalgo, H.G., Cayan, D.R., Swetnam, T.W., 2006. Warming and earlier spring increase western US fire activity. Science 313, 940–943.
Whitlock, C., Larsen, C.P.S., 2001. Charcoal as a fire proxy. In: Smol, J.P., Birks, H.J.B. (Eds.), Tracking Environmental Change Using Lake Sediments, Vol. 3, Terrestrial, Algal, and Siliceous Indicators. Kluwer Academic Publishers, Dordrecht, pp. 75–97.
Whitlock, C., Millspaugh, S.H., 1996. Testing the assumptions of fire-history studies: an examination of modern charcoal accumulation in Yellowstone National Park, USA. The Holocene 6, 7–15.
Whitlock, C., Bartlein, P.J., Marlon, J., Brunelle, A., Long, C., 2003. Holocene fire reconstructions from the northwestern U.S.: an examination at multiple timescales. Fifth Symposium on Fire and Forest Meteorology: American Meteorological Society.
Whitlock, C., Higuera, P.E., McWerthy, D.B., Briles, C.E., 2010. Paleoecological perspectives on fire ecology: revisiting the fire-regime concept. The Open Ecology Journal 3, 6–23.
Williams, A.P., Allen, C.D., Millar, C.I., Swetnam, T.W., Michaelsen, J., Still, C.J., Leavitt, S.W., 2010. Forest responses to increasing aridity and warmth in the southwestern United States. Proceedings of the North American Academy of Sciences 107, 211289–221294.
Willis, K.J., Birks, H.J.B., 2006. What is natural? The need for long-term perspective in biodiversity conservation. Science 314, 1261–1265.
Wilson, M.T., Thomas, H.E., 1964. Hydrology and hydrogeology of Navajo Lake, Kane County, Utah: U.S. Geological Survey Professional Paper 417-C (26 pp.).
Wise, E., 2010. Spatiotemporal variability of the precipitation dipole transition zone in the western United States. Geophysical Research Letters 37 http://dx.doi.org/10.1029/2009GL042193.
Zhao, Y., Harrison, S.P., 2011. Mid-Holocene monsoons: a multi-model analysis of the inter-hemispheric differences in the responses to orbital forcing and ocean feedbacks. Climate Dynamics http://dx.doi.org/10.1007/s00382-011-1193-z.
Zhao, Y., Liu, H., Li, F., Huang, X., Sun, J., Zhao, W., Herzschuh, U., Yu, T., 2012. Application and limitations of the *Artemisia*/Chenopodiaceae pollen ratio in arid and semi-arid China. The Holocene http://dx.doi.org/10.1177/0959683612449762.